PHYSICAL REVIEW B VOLUME 25, NUMBER 12 15 JUNE 1982

Quantum-mechanical-model calculations of radiative properties of a molecular crystal. I. Polaritons and abnormal decays of excitons in one- and two-dimensional systems

Michel Orrit, Claude Aslangul,* and Philémon Kottis
Centre de Physique Moléculaire, Optique et Hertzienne,† University of Bordeaux I, 33405 Talence, France and Centre de Mecanique Ondulatoire Appliqueé, 23, Rue du Maroc, 75019, Paris, France
(Received 31 January 1980; revised manuscript received 23 October 1981)

An analysis of the interaction of an electronic collective excitation, of dimensions 1 and 2, with the radiation field is presented. The use of translation symmetry in infinite lattices allows us to reduce the interaction problem to a coupling of a discrete matter state to an effective continuum of photons presenting a low-energy edge. The resulting states (radiatively unstable excitons, polaritons) are investigated as a function of the electronic excitation energy relative to the edge of the continuum, with emphasis on the spectral properties and the dynamical regimes in the intermediate region, when the energy of the electronic excitation sweeps the edge of the continuum. Contact with the three-dimensional polariton is made while application to radiative dynamics in layered crystals is suggested.

I. INTRODUCTION

The purpose of this series of papers is to present a quantum-mechanical model for the interaction of an ordered, weakly coupled, one-, two- or three-dimensional system with the radiation field, in the absence of phonons. An example of these systems will be a molecular chain, a plane of molecules, or a real finite crystal of layered structure interacting with a photon continuum. In this paper, we restrict our attention to the case where a discrete state of energy $\hbar\omega_0$ and wave vector $\vec{K}$, for example $|\vec{K}\rangle$, strongly couples to a continuum of photons. We analyze the effect of dimensionality on the states of the matter-radiation systems and we point out the conditions for instability as a function of the position of the discrete energy level $|\vec{K}\rangle$ relative to the photon continuum energy. These investigations allow a natural transition from the three-dimensional polariton limit introduced by Hopfield[1] and other authors[2] to one- and two-dimensional cases. One- and two-dimensional lattices have already been investigated quantum-mechanically by Agranovitch *et al.*[3] and classically by Philpott *et al.*[4–6] in what may be termed the pole approximation limit. We present an approach which goes beyond the pole approximation limit and allows us to investigate the behavior of the excitation in the intermediate regimes ($K \simeq \omega_0/c$) around the intersection of the two zero-order dispersion curves, for the so-called intermediate states between quasiphotons and quasiexcitons.

The major features of our approach can be outlined as follows: First, we solve the exact total Hamiltonian and calculate the eigenstate spectrum which contains the stable polariton, the unstable exciton, and perturbed photon states. Second, by calculating exactly the evolution of the amplitude $A_K(t)$ of the $|\vec{K}\rangle$ state and its Fourier transform $A_K(\omega)$, we analyze the excitation dynamics. We find that the dynamics of these coupled systems vary continuously and exhibit large variations in the decay characteristics of the discrete $|\vec{K}\rangle$ state (i.e., an exponential decay, oscillatory behavior, etc.). We should point out that it will not be possible to handle some of these dynamical regimes (especially the intermediate case) using the well-known pole approximation which is based on a perturbative approach. These new findings are important to the problem of crystal-surface excitation dynamics where a surface exciton couples to a crystal bulk continuum and to a radiation field, as examplified in the case of anthracene crystal on the *ab* surface,[6,7] as well as for bulk dynamics which will be presented in the second paper of this series.

The present paper is outlined as follows: In Sec. II we present our model and discuss its limitations; in Sec. III we define the basis of our mathematical approach. We discuss the weakness of the resonance approximation and introduce Feynman

propagators, which provide a better analytical behavior and suppress divergences of the matter-radiation coupling at low- and high-frequency limits. In Sec. IV, we present calculations of dispersion curves for one- and two-dimensional lattices; in addition, we provide detailed calculations for the excitation dynamics and of the smearing out of the matter state due to its coupling to the effective continuum of photons. Finally, in Sec. V, we use Feynman propagators both for photons and excitons and, as a test of our method of treating one- and two-dimensional lattices, we derive the well-known equation for three-dimensional polariton energies. We mention briefly the equivalence of the quasiboson approximation with the method of Feynman propagators, considered also by other authors particularly in the coupling of electrons with bosons (photons or phonons).[8]

II. DESCRIPTION OF THE MODEL

A. General definitions

The systems we are considering are infinite lattices of one or two dimensions. We replace the molecules by point dipoles placed at their centers. The dipoles we are considering are electric transition dipoles connecting the ground state to an excited state; this two-level approximation suffices for the investigation of phenomena near resonance. As a further approximation we restrict our attention to rigid lattices and we deal only with the excitonic and photonic components of the phenomena, neglecting phonon effects. Therefore, we keep in mind that important discrepancies may be expected when comparing our results with experimental data which may contain effects owing to, for instance, (i) renormalization of states by coupling to the thermal bath phonons, leading to shift and damping of the excitonic component of the polariton,[9] and (ii) damping from the formation of two-particle states[10] (exciton and phonon) continuum which may relax the vibronic excitons.

B. The Hamiltonian of the matter-radiation system

The interaction Hamiltonian is set up from the interaction of one molecule with the radiation field and its form will be common to all cases we are considering. The total Hamiltonian is given the usual form

$$H=H_m+H_r+H_I \ , \tag{1}$$

here the indices m, r, and I stand for matter, radiation, and interaction.

1. The matter Hamiltonian

The excited state of each lattice site $\vec{n}$ is written as $|\vec{n}\rangle$. When taking into account quantum exchange of excitation between different sites to form Frenkel excitons, one writes

$$H_m=\hbar\omega_0\sum_{\vec{n}}|\vec{n}\rangle\langle\vec{n}|+{\sum_{\vec{n},\vec{n}'}}' J_{\vec{n},\vec{n}'}|\vec{n}\rangle\langle\vec{n}'| \ , \tag{2}$$

where $\hbar\omega_0$ is the resonance energy of local transition and $J_{\vec{n},\vec{n}'}$ is the matrix element of the electrostatic dipolar interaction between sites $\vec{n}$ and $\vec{n}'$. H_m is diagonalized by Fourier transformation on the lattice-site states, using Born—von Kármán periodic boundary conditions,

$$H_m=\sum_{\vec{K}}\hbar\omega_K|\vec{K}\rangle\langle\vec{K}| \ , \tag{3}$$

with

$$|\vec{K}\rangle=\frac{1}{\sqrt{N}}\sum_{\vec{n}}\exp(i\vec{K}\cdot\vec{n})|\vec{n}\rangle$$

and

$$\hbar\omega_K=\hbar\omega_0+J(\vec{K}) \ . \tag{4}$$

$\vec{K}$ is the excitonic wave vector in the first Brillouin zone ($0\le K\le\pi/a$), $J(\vec{K})$ is the excitonic energy dispersion with

$$J(\vec{K})={\sum_{\vec{n}}}'\exp(i\vec{K}\cdot\vec{n})J_{0,\vec{n}} \ ,$$

and a indicates the lattice spacing. In problems of effective coupling with radiation, we have to consider only small values of excitonic wave vectors $K\ll\pi/a$, so that in what follows we may ignore the excitonic dispersion which may be included in the unperturbed energy of the exciton.

2. The radiation Hamiltonian

As usual, the radiation field is quantized in a box of side L where L goes to ∞; the field states are written $|\vec{k},\vec{\epsilon}\rangle$ with $\vec{k}\cdot\vec{\epsilon}=0$, where $\hbar\vec{k}$ and $\vec{\epsilon}$ are the momentum and the polarization of the photon. The wave vectors $\vec{k}$ form a three-

dimensional lattice with a constant spacing $(2\pi)/L$. This leads to the expression,

$$H_r=\hbar\sum_{\vec{k},\vec{\epsilon}}\omega_{\vec{k}}(a^{\dagger}_{kvec\epsilon}a_{\vec{k}\epsilon}+\tfrac{1}{2}) , \tag{5}$$

with

$$[a_{\vec{k}\epsilon},a^{\dagger}_{\vec{k}'\epsilon'}]=\delta_{\vec{k}\epsilon,\vec{k}'\epsilon'}$$

and

$$\hbar\omega_{\vec{k}}=\hbar c\,|\vec{k}| .$$

3. *The interaction Hamiltonian*

In order to derive the matter-radiation interaction we use the continuous medium approximation, which means that we neglect in the summation on the reciprocal lattice all the wave vectors which do not belong the first Brillouin zone. [See Eq. (8b).] This approximation is equivalent to neglecting the local-field contribution or, more precisely, its dispersion, since the contribution of the local field for $K=0$ may be assumed to be included in the excitonic energy $\hbar\omega_0$. This approximation is valid since we limit ourself to excitonic wave vectors $K\ll\pi/a$. (See Sec. II B 1 above.)

We now consider in detail the way the continuous medium approximation appears in the terms of the usual interaction Hamiltonian, which is built up by summation over all the charges α:

$$H_I=-\sum_{\alpha}\frac{e_\alpha}{m_\alpha}\vec{P}_\alpha\cdot\vec{A}(\vec{R}_\alpha)+\sum_{\alpha}\frac{e_\alpha^2}{2m_\alpha}\vec{A}^2(\vec{R}_\alpha) . \tag{6}$$

When giving to $\vec{A}$ its development on the radiation field modes, Eq. (6) transforms, when neglecting the term in A^2, to

$$H_I=-\sum_{\vec{k}\epsilon,\vec{n}}\frac{e}{m}\left[\frac{2\pi\hbar c^2}{L^3}\right]^{1/2}\frac{1}{\sqrt{\omega_{\vec{k}}}}\times\vec{P}_n\cdot\vec{\epsilon}(a_{\vec{k}\epsilon}e^{i\vec{k}\cdot\vec{n}}+a^{\dagger}_{-\vec{k}\epsilon}e^{-i\vec{k}\cdot\vec{n}}) . \tag{7a}$$

$\vec{P}_n$, which is the momemtum operator of the nth cell of the matter system, is related to the electric transition dipole $\vec{D}_n$ (the index n is dropped since all the dipoles $\vec{D}_n$ are parallel) as follows:

$$\vec{P}_n=\frac{im\omega_0}{e\hbar}(|n\rangle\langle 0|-|0\rangle\langle n|)\vec{D} . \tag{7b}$$

Also, denoting by $\vec{P}_K$ the momentum operator of the matter system,

$$\vec{P}_{\vec{K}}=\frac{im\omega_0}{e\hbar}(|\vec{K}\rangle\langle 0|-|0\rangle\langle\vec{K}|)\vec{D} , \tag{7c}$$

we may use the Fourier transformation

$$\vec{P}_n=N^{-1/2}\sum_K e^{-i\vec{K}\cdot\vec{n}}\vec{P}_{\vec{K}}$$

in order to eliminate the site variables in (7a) which becomes

$$H_I=-\sum_{\vec{k}\epsilon,K}\frac{e}{m}\left[\frac{2\pi\hbar c^2}{L^3}\right]^{1/2}\frac{\sqrt{N}}{\sqrt{\omega_{\vec{k}}}}\times\left[\frac{1}{N}\sum_n e^{i\vec{k}\cdot n_e-i\vec{K}\cdot\vec{n}}\right]\times\vec{P}_K\cdot\vec{\epsilon}(a_{\vec{k}\epsilon}+a^{\dagger}_{-\vec{k}\epsilon}) . \tag{8a}$$

In order to benefit from selection rules of the momentum conservation law, let us decompose the three-dimensional photon vector $\vec{k}$ into a component $\vec{k}_{||}$ lying in the matter subspace, and a component $\vec{q}$ orhtogonal to it, i.e., $\vec{k}=\vec{k}_{||}+\vec{q}$. Using this decomposition, the summation $\sum_n$ in Eq. (8a) transforms to

$$\frac{1}{N}\sum_n e^{i(\vec{k}-\vec{K})\cdot\vec{n}}=\frac{1}{N}\sum e^{i(\vec{k}_{||}-\vec{K})\cdot\vec{n}}=\sum_{\vec{G}}\delta(\vec{k}_{||}-\vec{K}+\vec{G}) , \tag{8b}$$

where $\sum_G$ extends over all reciprocal-lattice vectors of the matter system. Neglecting the terms $\vec{G}\neq 0$, i.e., "umklapp" processes, is equivalent to neglecting the atomic character of the matter and making the jellium approximation. Therefore, the approximation $\vec{G}=0$ provides the selection rule $\vec{k}_{||}=\vec{K}$ which simplifies the interaction Hamiltonian to

$$H_I^K=-\sum_{\vec{q}\epsilon,K}\frac{e}{m}\left[\frac{2\pi\hbar c^2}{L^3}\right]^{1/2}\times\left[\frac{N}{\omega_k}\right]^{1/2}\vec{P}_K\cdot\vec{\epsilon}(a_{k\epsilon}+a^{\dagger}_{k\epsilon}) , \tag{8c}$$

with $\vec{k}=\vec{K}+\vec{q}$. The summation over photon states now involves only the component $\vec{q}$ which is of lower dimension than three and defines the effective continuum to which the exciton $\vec{K}$ is effectively coupled. In fact, the subspace of the $\vec{q}$'s is

complementary to the subspace of $\vec{K}$ in the sense that if we indicate, respectively, by $\mathscr{D}_q$ and $\mathscr{D}_K$ the dimension of these two subspaces, we have $\mathscr{D}_q=3-\mathscr{D}_K$. Using the translational invariance of the lattice and the interaction Hamiltonian given by (8c), it is straightforward to diagonalize the total Hamiltonian by blocks of total momentum $\vec{K}$.

4. *Dimensionality effects and nature of the effective continuum*

In each subspace $\vec{K}$ the interaction problem amounts to the investigation of the coupling of the discrete state $|\vec{K};0\rangle$ to the continuum of photon states $|0;\vec{K}+\vec{q},\vec{\epsilon}\rangle_{0\le q<\infty}$. In what follows, we analyze the structure of this continuum for each dimension.

(*i*) *Zero dimension.* In this case one point dipole is coupled to a three-dimensional continuum of photons. It is well known that in this case one obtains a radiative shift and a radiative width as well as a nonexponential contribution to the radiative decay at long times. The effective continuum is three-dimensional with a density of states $g^{(0)}(\omega)$ which is a "smooth function" of ω:

$$g^{(0)}(\omega)=\frac{L^3}{2\pi^2c^3}\omega^2 . \tag{9a}$$

(*ii*) *One dimension.* The lattice is a chain of molecules and $\vec{K}$ defined by the chain is one-dimensional. It is coupled to the continuum of photons $\vec{k}=(\vec{K}+\vec{q})_{0\le\vec{q},\infty}$, $\vec{q}$ being perpendicular to the chain. The effective continuum is two-dimensional with a density of states,

$$g^{(1)}(\omega)=\begin{cases}\dfrac{L^2}{2\pi c^2}\omega & \text{for } \omega>cK\\ 0 & \text{for } \omega<cK.\end{cases} \tag{9b}$$

This exhibits a discontinuity at $\omega=cK$ for which anomalous decay of $|\vec{K};0\rangle$ is expected for excitonic energies $\hbar\omega_0\simeq\hbar cK$.

(*iii*) *Two dimensions.* The lattice is a plane of molecules; $\vec{K}$ is two-dimensional and lies in the plane. It is coupled to the continuum of photons $\vec{k}=(\vec{K}+\vec{q})_{0\le\vec{q}<\infty}$ whose component $\vec{q}$ is carried by a line normal to the plane. The effective continuum is one-dimensional with a density of states,

$$g^{(2)}(\omega)=\begin{cases}\dfrac{L}{2\pi c}\dfrac{\omega}{(\omega^2-c^2K^2)^{1/2}} & \text{for } \omega>cK\\ 0 & \text{for } \omega<cK.\end{cases} \tag{9c}$$

It exhibits a singularity and diverges for $\omega=cK$.

(*iv*) *Three dimensions.* The lattice occupies the whole space of quantization of the photons, the matter state $|\vec{K};0\rangle$ no longer faces a continuum of photons but it is coupled to a single photon with $\vec{k}=\vec{K}$, and the density of states is reduced to a Dirac function $\delta(\vec{K}-\vec{k})$.

In general, when matter excitations are coupled to a continuum of photons, these states are radiatively unstable. Furthermore, a singularity in the continuum near the critical point $K_0=\omega_0/c$ gives rise to a complex radiative decay the nature of which will be examined below.[11]

Before concluding this section we would like to remind the reader that these considerations may be generalized to systems other than Frenkel excitons, provided that the interaction involves only two types of particles, photon-exciton such as in ionic crystals, photon-optical phonon, etc.

III. CHOICE OF THE MATHEMATICAL APPROACH

A. Introduction

When a discrete state is coupled to a continuum, the spectrum of the "new" eigenstates is still continuous, with possibly discrete states split off at the edges of the continuum. These discrete states are characterized by their energy, while the states of the continuum may be characterized (i) by the restriction of the resolvent $G(z)$ to the initial discrete state, or (ii) equivalently and in a more general way, by the scattering amplitude between states of the initial continuum (S matrix elements). In part C of this section, we discuss these two approaches. Now, with the reduced interaction (8c) we are led to investigate the coupling of a discrete excitonic state $|\vec{K}\rangle$ to a continuum of photons $(\vec{K}+\vec{q})_{0\le q<\infty}$, cf. Eqs. (9). However, in addition to resonant processes, the interaction H_I^K couples by antiresonant processes, the state $|\vec{K};0\rangle$ to states $|\vec{K},\vec{K};-\vec{K}+\vec{q},\vec{\epsilon}\rangle$ with two excitons and one photon,[12] and then, by the successive powers of H_I, to states containing a higher and higher number of excitons and photons. Therefore, if we are not able to sum up all the processes of the perturbation, it is necessary to truncate to a given order the sub-

space Q of states accessible from $|\vec{K};0\rangle$, with the subsequent difficulty of this task. We may overcome this difficulty by a renormalization of the photonic propagator which allows us to treat both resonant and antiresonant processes.

B. Restriction of the resolvent in the matter subspace

1. General formalism

In a general way[13] the space of the states of the matter-radiation system is partitioned into two orthogonal subspaces with projectors P and Q which satisfy

$$P+Q=1, \quad PQ=QP=0 .$$

The restriction of the resolvent $G(z)=(z-H)^{-1}$ to the subspace P is written $PG(z)P$. The total Hamiltonian is written as $H=H_0+H_I$. Because P and Q are eigenspaces of H_0, and H_I couples P to Q, one has the general relations:

$$G=G_0+G_0H_IG ,$$

$$PGP=PG_0P+PG_0H_IPGP+PG_0H_IQGP ,$$

$$QGP=QG_0H_IPGP+QG_0H_IQGP ,$$

with

$$G_0=(z-H_0)^{-1} .$$

The elimination of QGP leads to the restricted resolvent

$$PGP=P[(PG_0P)^{-1}-PR(z)P]^{-1} . \tag{10a}$$

The so-called self-energy PRP has the following expression

$$PR(z)P=PH_IP+PH_IQ\frac{1}{z-QHQ}QH_IP . \tag{10b}$$

In our specific system we always have $PH_IP=0$.

2. The resonance approximation

The only elementary process we consider involves states with only one photon. Then the projectors to be considered are

$$P=|\vec{K};0\rangle\langle\vec{K};0|$$

and

$$Q=\sum_{q\epsilon}|0;\vec{K}+\vec{q},\vec{\epsilon}\rangle\langle 0;\vec{K}+\vec{q},\vec{\epsilon}| .$$

With the use of interaction (8c), where we replace $\vec{P}_K$ by (7c), the operator (10b) is a function with the explicit form

$$R_r(z)=\frac{2\pi N\hbar}{L^3}\sum_{\vec{q}\,\vec{\epsilon}}\frac{\omega_0^2}{\omega_{\vec{K}+\vec{q}}}(\vec{\epsilon}\cdot\vec{D})^2\frac{1}{z-\hbar\omega_{K+q}} . \tag{10c}$$

The resonance approximation sums up in PGP all the powers of H_I in the subspaces P and Q. Nevertheless, because of the divergence at $\omega_k\to 0$ of the interaction (10c) for certain dimensions of the continuum, an artificial cutoff function must be introduced for low frequencies.

3. Feynman propagators

We replace the photonic propagator $1/(z-\hbar\omega_{K+q})$ in the resonance approximation (10c) by the Feynman propagator

$$2\hbar\omega_{K+q}/[z^2-(\hbar\omega_{K+q})^2] .$$

Although this change causes negligible effects near resonance ($z=\hbar\omega_{K+q}$), it provides a much simpler analytical expression for the interaction. In particular, the presence of antiresonant terms in the Feynman propagator suppresses the infrared divergence which appears in (10c) for a two-dimensional lattice. With the Feynman propagator, the self-energy (10c) has the form

$$R_F(z)=\frac{4\pi N\hbar^2}{L^3}\omega_0^2\sum_{\vec{q}\,\vec{\epsilon}}(\vec{\epsilon}\cdot\vec{D})^2\frac{1}{z^2-(\hbar\omega_{K+q})^2} . \tag{11}$$

In what follows, we consider R_F as the complete self-energy and write it as R.

C. The dynamics of the matter state coupled to the photon continuum

1. The time evolution of the initial state

We look for the probability of finding the system in the initial matter state $|\vec{K}\rangle$ at a later time t, the amplitude of this probability being

$$A_K(t)=\langle\vec{K}|U(t)|\vec{K}\rangle , \tag{12}$$

with

$$U(t)=-\frac{1}{2i\pi}\times\int_{C_+}\exp(-izt/\hbar)G(z)d(z)\ .$$

The path of integration is

$$C_+=[-\infty+i\epsilon,+\infty+i\epsilon]$$

as shown in Fig. 1; the region $[cK<z<\infty]$ constitutes a cut for $G(z)$. As shown in Fig. 1, the amplitude (12) contains two contributions, that from the poles of $G(z)$ and that from an integral $L_K(t)$, which is generally much smaller than the contribution from the poles except in the intermediate region ($K\simeq\omega_0/c$). $L_K(t)$ becomes important and secures the continuity of $A_K(t)$ vs K, when K crosses the intermediate region. Thus one can write (res indicates residues),

$$A_K(t)=\sum\text{res}+L_K(t)\ , \tag{13}$$

with

$$L_K(t)=\frac{1}{2\pi i}\left[\int_{cK-i\infty}^{cK}\exp(-izt/\hbar)G_K(z)dz+\int_{cK}^{cK-i\infty}\exp(-izt/\hbar)G_K(z)dz\right]\ ,$$

and

$$G_K(z)=\langle\vec{K}\,|\,G(z)\,|\,\vec{K}\rangle\ .$$

When only one pole contributes significantly, the evolution is an exponential decay. On the other hand, when two or more poles contribute, or when the integral over the loop $L_K(t)$ (cf. Fig. 1) is important, then the evolution is more complex, as shown below in Figs. 10 and 11.

2. *Spectral broadening of the matter state*

The Fourier transform $A_K(\omega)$ of $A_K(t)$ provides the probability of finding the energy $\hbar\omega$ at the end of the decay. Using the relations

$$\int_{-\infty}^{+\infty}G_K(\omega-i0)\exp(izt/\hbar)\,dz=0\ , \tag{14}$$

$$A_K(t)=\frac{\hbar}{2\pi i}\int_{-\infty}^{+\infty}[G_K(\omega-i0)-G_K(\omega+i0)]\times\exp(-i\omega t)\,d\omega\ ,$$

and the explicit expressions

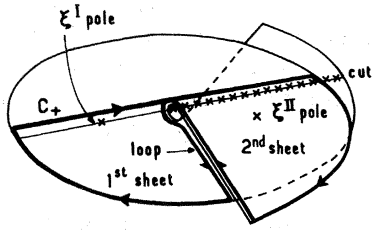

FIG. 1. The integral (35) must be taken along the line C_+. In order to get the experimental decay from the complex ξ^{II} pole, it is necessary to close the integration contour. However, this may be done only by passing from the second sheet to the first one, for instance, by means of a loop parallel to the imaginary axis. The contribution of the loop, although small for $cK<\omega_0$ and $cK>\omega_0$, becomes quite comparable to that of the ξ^{II} pole in the intermediate region $cK\simeq\omega_0$.

$$G_K(\omega\pm i0)=[\hbar(\omega-\omega_0)-R_K(\omega\pm i0)]^{-1}\ ,$$
$$R_K(\omega\pm i0)=\hbar\left[\Delta_K(\omega)\pm\frac{i}{2}\Gamma_K(\omega)\right]\ , \tag{15}$$

we arrive at the Fourier transform

$$A_K(\omega=\frac{1}{2\pi}\int_{-\infty}^{+\infty}A_K(t)\exp(-i\omega t)\,dt$$
$$=\frac{1}{2\pi}\frac{\Gamma_K(\omega)}{[\omega-\omega_0-\Delta_K(\omega)]^2+\frac{1}{4}\Gamma_K(\omega)^2}\ . \tag{16}$$

Using the basis $|i\rangle$ of the eigenstates of H and their density $g(\omega)$ [cf. (9)] at the energy $\hbar\omega$, we may write

$$A_K(\omega)=|\langle\vec{K}\,|\,i\rangle|^2 g(\omega)\ . \tag{17}$$

If the spectrum of H contains discrete states, then $A_K(\omega)$ contains Dirac peaks. As for the density of states $g(\omega)$ we use the functions (9), since this density is not modified by the coupling to a discrete state, with the exception of a possible splitting off of the lowest-energy state of the continuum,[14] cf. Fig. 2. $A_K(\omega)$ represents the spectral density of the matter state at the energy $\hbar\omega$. Owing to coupling

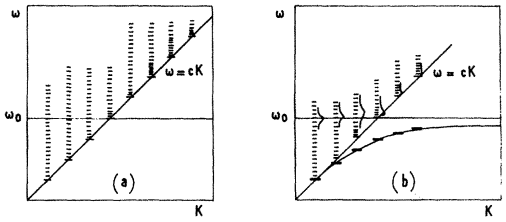

FIG. 2. Variation vs K of the edge of the effective continuum of photons. $\hbar\omega_0$ indicates the energy of the excitons discrete state. (b) the states below the edge cK are radiatively stable states (polaritons) and the states above the edge are the excitonic resonances in the effective continuum.

with the continuum, it represents also the population of the channel of energy $\hbar\omega$ following the decay of $|\vec{K}\rangle$. In addition, the expression

$$A_K(\omega)/g(\omega)=|\langle\vec{K}|i\rangle|^2$$

represents the matter component of the continuum. Its connection with the dimensionality is obvious and will be discussed below in the section of applications.

Concluding this section, let us indicate that the function $G_K(\omega+i0)$ allows the calculation of a more general expression than $A_K(\omega)$. This is the scattering matrix S:

$$\langle 0;\vec{K}+\vec{q},\vec{\epsilon}|S|0;\vec{K}+\vec{q}',\epsilon'\rangle=\delta_{qq'}\delta_{\epsilon\epsilon'}-\frac{2i\pi}{\hbar}\langle 0;\vec{K}+\vec{q},\vec{\epsilon}|H_I^K|\vec{K};0\rangle\langle\vec{K};0|H_I^K|0;\vec{K}+\vec{q}',\epsilon'\rangle$$

$$\times G_K(\omega_{K+q}+i0)\delta(\omega_{K+q}-\omega_{K+q'}),$$

which contains the full description of a continuum scattered by a lattice of electric transition dipoles. This expression allows one to calculate quantities such as reflectivity or transmission by a two-dimensional lattice, or light scattering by a molecular infinite chain.

IV. APPLICATIONS AND DISCUSSION

A. One-dimensional excitations coupled to the radiation

Let us first calculate the self-energy $R^{(1)}$. Using the density of states $g^{(1)}(\omega)$ [cf. (9b)] and writing $L=Na$, one derives from (11),

$$R^{(1)}(z)=\frac{(\hbar\omega_0)^2}{\pi a}\int\int d^2q\frac{\sum_\epsilon(\vec{\epsilon}\cdot\vec{D})^2}{[z^2-(\hbar\omega_{K+q})^2]}. \tag{18}$$

After summation over the polarization $\vec{\epsilon}$ perpendicular to $\vec{K}+\vec{q}$, angular integration, and writing $\omega_{K+q}=c(K^2+q^2)^{1/2}$, one obtains

$$R^{(1)}(z)=\frac{(\hbar\omega_0 D)^2}{a}\int_0^\infty q\,dq\frac{\left[1+\frac{K^2-(2K^2-q^2)\cos^2\theta}{K^2+q^2}\right]}{[z^2-(\hbar c)^2(K^2+q^2)]}F(K+q), \tag{19}$$

where θ is the angle between the axis of the molecular chain and the direction of the electric transition dipole $\vec{D}$. $F(K+q)$ is the usual cutoff phenomenological function which prevents the logarithmic divergence of (19) for $q\to\infty$ and secures the decrease of the dipole-radiation coupling for large values of q. In order to simplify (19), we take for $F(k)$ a Lorentzian form,

$$F(k)=\frac{1}{1+l^2k^2},$$

where l is a characteristic length of a molecule. For a standard calculation of (19) let us introduce dimensionless parameters such as:

$$K_0=\omega_0/c,\quad \xi=z/\hbar\omega_0,\quad \mu=(cK/\omega_0)=K/K_0\ ,$$
$$f=D^2/e^2a^2,\quad \alpha=e^2/\hbar c,\quad \eta=lK_0\ . \tag{20}$$

This transforms (19) into

$$R^{(1)}(\xi)=f\alpha\hbar\omega_0\frac{\omega_0 a}{c}\int_0^\infty x\,dx\frac{1+\dfrac{\mu^2-(2\mu^2-x^2)\cos^2\theta}{\mu^2+x^2}}{\xi^2-\mu^2-x^2}\frac{1}{1+\eta^2(\mu^2+x^2)}\ . \tag{21}$$

This expression has a cut extending from μ to ∞ on the real axis. After integration, one gets two solutions of $R^{(1)}(\xi)$, one noted $R^{(1)\mathrm{I}}$ in the first and one noted $R^{(1)\mathrm{II}}$ in the second Riemann sheet, with

$$R^{(1)\mathrm{I,II}}(\xi)=\hbar\omega_0\frac{f\alpha}{2}\frac{\omega_0 a}{c}\left[\left[\frac{\mu^2}{\xi^2}(1-3\cos^2\theta)+1+\cos^2\theta\right]\ln(\mu^2-\xi^2)\right.$$
$$\left.+(3\cos^2\theta-1)\frac{\mu^2}{\xi^2}\ln\mu^2+(1+\cos^2\theta)\ln\left[\frac{1}{\eta}+\mu^2\right]\right]\ . \tag{22}$$

$\ln(\mu^2-\xi^2)$ is such that we have for the two solutions:

$$\ln(\mu^2-\xi^2)=\begin{cases}\ln(x^2-\mu^2)-i\pi & \text{with } \xi^{\mathrm{I}}=x+i0 \text{ and } \mu<x\\ \ln(x^2-\mu^2)=i\pi & \text{with } \xi^{\mathrm{II}}=x-i0 \text{ and } \mu<x\ .\end{cases} \tag{23}$$

In (22) we notice the presence of the factor $aK_0=\omega_0 a/c$; on the other hand, the radiative width $\Gamma^{(0)}$ of a single dipole (system of zero dimension) would be, using the parameters (20),

$$\Gamma^{(0)}=\tfrac{4}{3}f\alpha\hbar\omega\left[\frac{\omega_0 a}{c}\right]^2\ .$$

Thus, with respect to the radiative width $\Gamma^{(0)}$ of a single dipole, the radiative width of a one-dimensional radiant exciton is multiplied by a factor $c/\omega_0 a$. This amplification factor, of an order 10^3 with typical values for ω_0 and a, may be interpreted as an emission in phase of λ/a dipoles of the chain, where λ is the emitted wavelength. Angular and K dependence of the radiative shifts are discussed below for the different approximations used.

1. The pole approximation

For a small shift $R(z)$ which varies slowly with z (as for an isolated dipole, for instance) one gets an excellent approximation of $G(z)$ be replacing z in $R(z)$ by $\hbar(\omega_0+i\epsilon)_{\epsilon\to 0}$

$$G_K(z)\simeq[z-\hbar\omega_0-R_K(\hbar\omega_0+i0)]^{-1}\ , \tag{24}$$

with the complex energy

$$\hbar\omega_0+R_K(\hbar\omega_0+i0)=\hbar\left[\omega_0+\Delta_K-\frac{i}{2}\Gamma_K\right]\ , \tag{25}$$

giving a strictly exponentially decaying evolution. The quantities Δ_K and Γ_K, the so-called frequency shift and radiative width, depend on the wave vector K. Substitution of $R_K^{(1)}$ in (22), and with $\eta\ll 1$ (10^{-3}), provides

$$\frac{\Delta_K}{\omega_0}=\alpha f a K_0\left[(1+\cos^2\theta)\ln(\eta^2|\mu^2-1|)\right.$$
$$\left.+\mu^2(1-3\cos^2\theta)\ln\frac{|\mu^2-1|}{\mu}\right]\ , \tag{26}$$

$$\frac{\Delta_K}{\omega_0}=-\Theta(1-\mu)2\pi\alpha f a K_0\,|\,1+\cos^2\theta$$
$$+\mu^2(1-3\cos^2\theta)\,|\ , \tag{27}$$

where Θ is the Heaviside function $\Theta(x>0)=1$ and $\Theta(x<0)=0$. The variations of Δ_K and Γ_K, as functions of K and in the pole approximation, are illustrated in Figs. 3 and 4.

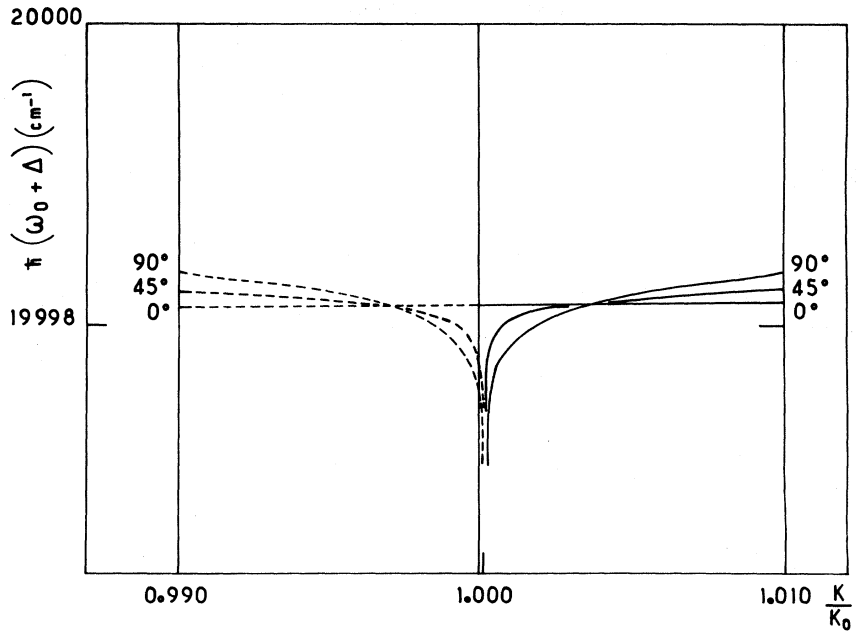

FIG. 3. One-dimensional states in the pole approximation: variation vs K of the energy for three angles θ between the electric transition dipole $\vec{D}$ and the lattice axis. Solid lines indicate the real poles and broken lines the real part of the complex poles. The quasivertical line indicates the edge $\hbar cK$ of the effective continuum. We notice a logarithmic divergence at $K \to K_0$.

2. *Calculations of the poles of the resolvent* $G_K(z)$

The next step is to calculate the poles of $G_K(z)$ in order to arrive at a more accurate derivation of the dynamics of the matter-radiation interaction

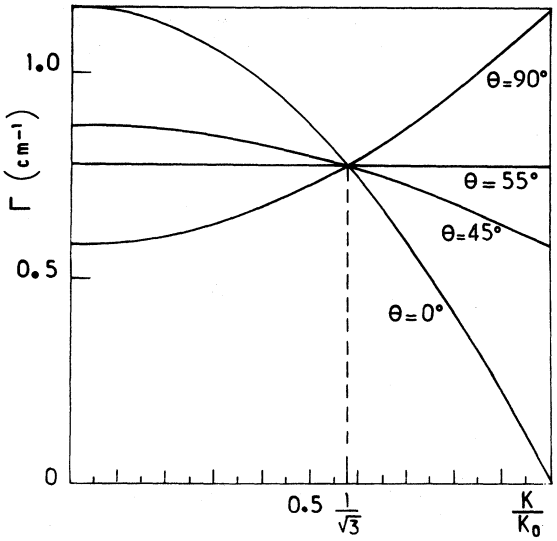

FIG. 4. One-dimensional states in the pole approximation: variation vs K of the radiative decay rate for four angles θ between the electric transition dipole $\vec{D}$ and the lattice axis. A discontinuity occurs at $K=K_0$, since for $K>K_0$ the decay rate is zero.

for all values of K (the dynamics are fully accounted for when we include the contribution of $L_K(t)$, [see (13)]. Equation (25) becomes now an implicit equation to be solved in each Riemann sheet

$$\xi_K^{\mathrm{I,II}} = 1 + \frac{1}{\hbar\omega_0} R_K^{\mathrm{I,II}}(\xi_K^{\mathrm{I,II}}) \,. \tag{28}$$

(I,II designate the first and second sheets.) According to the contour chosen, cf. Fig. 1, the poles in the second sheet contribute to the amplitude $A_K(t)$ only if their real part satisfies $\mathrm{Re}\,\xi_K^{\mathrm{II}} > (\hbar cK)/(\hbar\omega_0)$; otherwise their contribution is included in the integral $L_K(t)$, cf. (13).

We have calculated numerically the real and imaginary parts of $\hbar\omega_0\xi^{\mathrm{I}}$ and $\hbar\omega_0\xi^{\mathrm{II}}$, as a function of K and derived exact frequency shifts and radiative widths from the relation

$$\hbar\left[\Delta_K^{\mathrm{I,II}} - \frac{i}{2}\Gamma_K^{\mathrm{I,II}}\right] = \hbar\omega_0(\xi_K^{\mathrm{I,II}} - 1) \,. \tag{29}$$

The calculations are illustrated in Fig. 5.

B. Two-dimensional excitations coupled to the radiation

Let us first calculate the self-energy $R^{(2)}$. With $L = Na$, one derives from (11),

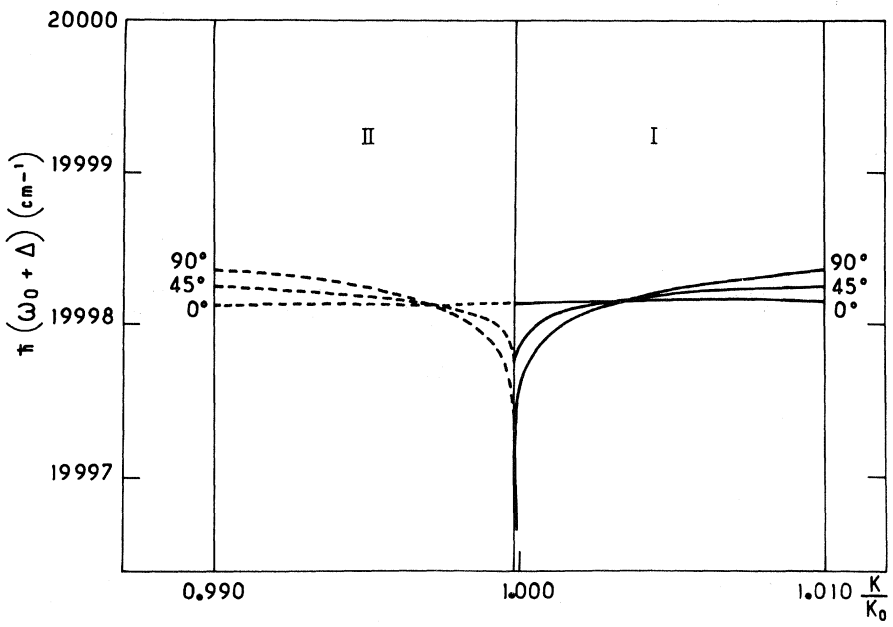

FIG. 5. One-dimensional states with the exact pole: variation of the energy vs K for three angles θ. In the first sheet (I) the poles are real (solid lines), they define eigenstates of H and give the dispersion of the polariton in the chain, In the second sheet (II) the poles are complex with real parts indicated by broken lines; they define radiatively unstable states. The quasivertical line indicates the edge photon $\hbar cK$ to which the solid lines are asymptotic.

$$R^{(2)}(z)=\frac{4\hbar}{a^2c}(\omega_0 D)^2\int_0^\infty dq\frac{1-\dfrac{K^2}{K^2+q^2}\cos^2\theta}{z^2-\hbar^2c^2(K^2+q^2)}\ . \tag{30}$$

To simplify, the dipole $\vec{D}$ was assumed to lie in the plane and to make an angle θ with the excitonic momentum $\vec{K}$. We notice that (30) converges without need of a cutoff function; this property is specific to dimension two. Also the divergence for $K\to 0$, present in the resonance approximation, is naturally eliminated with the use of Feynman propagators. With the dimensionless parameters (20), we obtain for the solutions $R^{\mathrm{I,II}}$ in the first and second Riemann sheet,

$$R^{(2)\mathrm{I,II}}(\xi)=2\pi f\alpha\hbar\omega_0\left[-\frac{\mu^2}{\xi^2}\cos^2\theta-\frac{i}{(\xi^2-\mu^2)^{1/2}}\left[1-\frac{\mu^2}{\xi^2}\cos^2\theta\right]\right]. \tag{31}$$

The complex square root is chosen so that R^{I} corresponds to $(\xi^2-\mu^2)^{1/2}=i(\mu^2-x^2)^{1/2}$ for $\xi=x+i0$ with $\mu>x$, and R^{II} corresponds to $(\xi^2-\mu^2)^{1/2}=(x^2-\mu^2)^{1/2}$ for $\xi=x+i0$ with $\mu<x$.

1. *The pole approximation*

Following the same procedure as for the one-dimensional case, one derives for the radiative shifts:

$$\Delta_K=\begin{cases}2\pi f\alpha\omega_0\left[-\mu\cos^2\theta-\dfrac{1-\mu^2\cos^2\theta}{(\mu^2-1)^{1/2}}\right] & \text{for } \mu>1\ ,\\ 2\pi f\alpha\omega_0(-\mu\cos^2\theta) & \text{for } \mu<1\ ,\end{cases} \tag{32}$$

$$\Gamma_K = \begin{cases} 0 \text{ for } \mu > 1 \\ 4\pi f \alpha \omega_0 \dfrac{1-\mu^2\cos^2\theta}{(1-\mu^2)^{1/2}} \text{ for } \mu < 1 \end{cases} . \tag{33}$$

The variation of Δ_K and Γ_K as functions of $\vec{K}$, are illustrated in Figs. 6 and 7 for several angles θ.

2. *Calculation of the poles of the resolvent*

Numerical solution of the implicit equations

$$\xi_K^{\mathrm{I,II}} = 1 + \frac{1}{\hbar\omega_0} R_K^{\mathrm{I,II}}(\xi^{\mathrm{I}}, \xi^{\mathrm{II}}) ,$$

(I,II designates first and second sheet) allowed us to derive exact values for the frequency shifts $\Delta^{\mathrm{I,II}}(K)$ and the radiative widths $\Gamma^{\mathrm{I,II}}(K)$. The results are illustrated in Figs. 8 and 9, respectively.

C. Exact calculation of $A_K^{(j)}(t)$ and generalization of the polariton concept

According to the value K, the amplitude (13) takes the following expression:

$$A_K^{(j)}(t) = \begin{cases} \mathrm{res}^{\mathrm{I}} + \mathrm{res}^{\mathrm{II}} + L_K & \text{for } K < K_{\mathrm{cr}} \\ \mathrm{res}^{\mathrm{I}} + L_K & \text{for } K > K_{\mathrm{cr}} , \end{cases} \tag{34}$$

where $cK_{\mathrm{cr}} = \omega_0 + \Delta(K_{\mathrm{cr}})$, K_{cr} indicates the critical value beyond which ($K > K_{\mathrm{cr}}$) $\mathrm{res}^{\mathrm{II}}$ has no physical meaning (cf. Figs. 8 and 9), its contribution being included in L_K. In what follows the treatment is common to one- and two-dimensional systems: $j = 1,2$ indicates the dimension and the corresponding self-energy, respectively, (19) and (30), which we are introducing in the calculation of (34).

In fact, no discontinuity appears in the amplitude (34) when K crosses K_{cr}, because the absence of $\mathrm{res}^{\mathrm{II}}$ is compensated by the integral

$$L_K(t) = -\frac{1}{2i\pi} \int_{cK/\omega_0 - i\infty}^{cK/\omega_0 - i0} \left[\frac{1}{\xi - 1 - \dfrac{R^{\mathrm{I}}(\xi)}{\hbar\omega_0}} - \frac{1}{\xi - 1 - \dfrac{R^{\mathrm{II}}(\xi)}{\hbar\omega_0}} \right] e^{-i\xi\omega_0 t} d\xi , \tag{35}$$

which changes suddenly on the passage of the pole to the other side of the loop (cf. Fig. 1).

From the calculation of the residues in (34), one obtains

$$\mathrm{res}^{\mathrm{I,II}} = e^{-i\xi^{\mathrm{I,II}}\omega_0 t} \left[1 - \frac{1}{\hbar\omega_0} \frac{dR^{\mathrm{I,II}}}{d\xi} \bigg|_{\xi^{\mathrm{I}}, \xi^{\mathrm{II}}} \right] . \tag{36}$$

The numerical integration of $L_K(t)$ is delicate but we have the check $A_K(0) = 1$. The results of the calculation of (34) are illustrated in Figs. 10 and 11. They satisfy the relation $|A_K(0)| = 1$ with an accuracy better than 10^{-4} for the real part and better than 5×10^{-3} for the imaginary part. Because of the strong decay of $e^{-i\xi\omega_0 t}$, the integral $L_K(t)$ provides a significant contribution only in the intermediate region; elsewhere, the calculation of $A_K(t)$ is satisfactory with only the contribution of the poles:

$$A_K(t) = \begin{cases} e^{-i(\omega_0 + \Delta_K^{\mathrm{II}})} e^{-\Gamma_K^{\mathrm{II}} t}, & 0 < K \ll K_0 \\ e^{-i(\omega_0 - \Delta_K^{\mathrm{I}})t}, & K \gg K_0 . \end{cases} \tag{37}$$

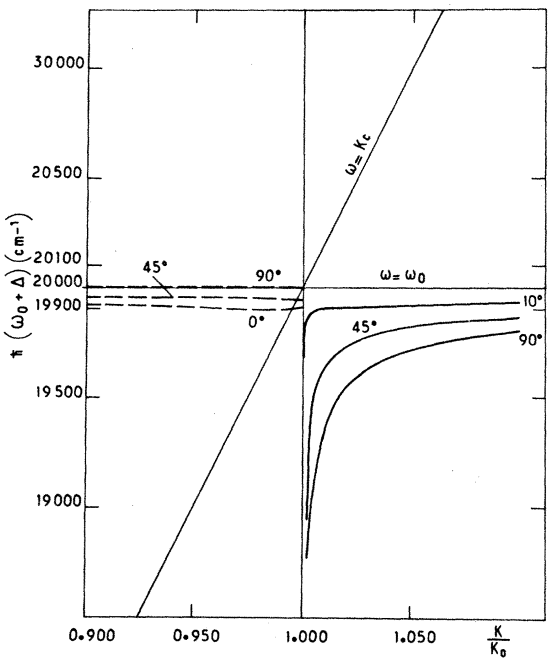

FIG. 6. Two-dimensional states in the pole approximation: variation vs K of the energy for different angles θ between the transiton dipole $\vec{D}$ and the wave vector $\vec{K}$. Solid lines indicate the real poles and broken lines the real parts of the complex poles. The line $\omega=cK$ indicates the variation of the edge of the effective continuum.

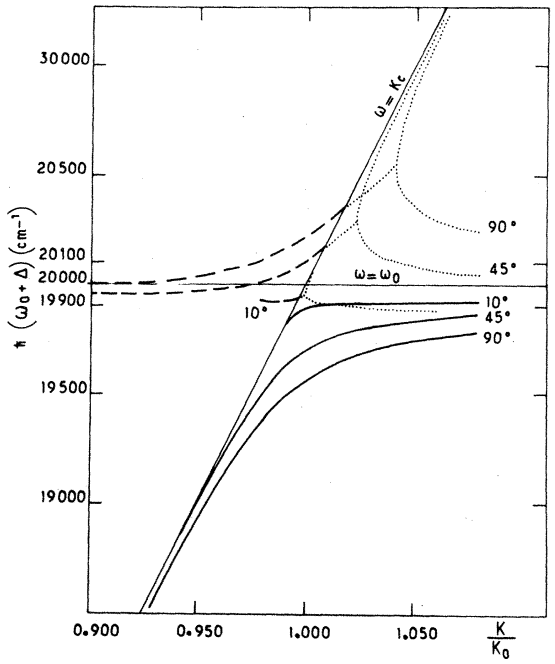

FIG. 8. Two-dimensional states with exact poles: variation of the energy vs $\vec{K}$ for three angles θ. Solid lines indicate the real poles (polariton), broken lines indicate the real parts of the complex poles (unstable excitons), and dotted lines indicate branches without physical meaning.

In the intermediate region, cf. Figs. 10 and 11, the two poles and the integral contribute and the behavior of $A_K(t)$ is no longer simple; it shows oscillations which, unlike the three-dimensional po-

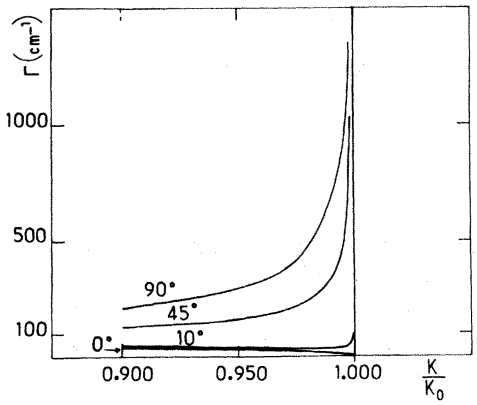

FIG. 7. Two-dimensional states in the pole approximation: variation vs K of the radiative decay rate for different angles θ. The rate diverges for $K\rightarrow K_0$ with $K<K_0$.

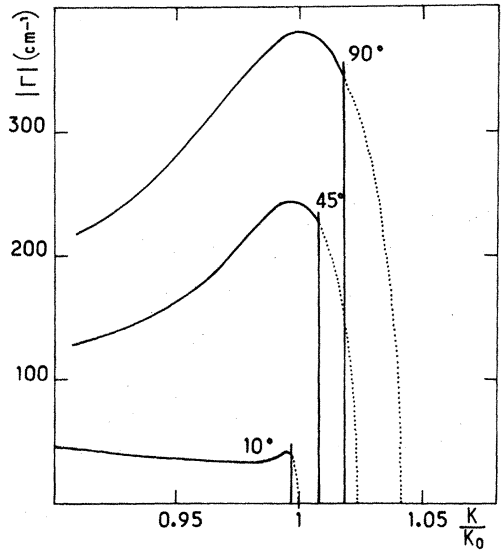

FIG. 9. Two-dimensional states with exact poles: variation vs $\vec{K}$ of the radiative decay rate for different angles θ. The divergences are eliminated; dotted lines indicate branches without physical meaning.

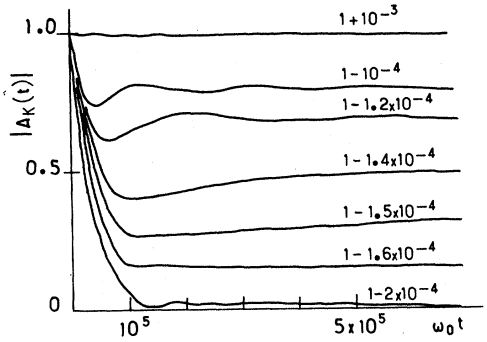

FIG. 10. One-dimensional states: variation of the modulus of the probability amplitude $a_k(t)$ for different values of the ratio K/K_0 in the intermediate region. The time scale of the decay is of the order of 10^{-10} sec.

lariton, are damped because of the presence of the effective continuum.

Now, we wish to show that a Fourier analysis of $A_K(t)$ leads, in a simple manner, to the derivation of radiatively stable states and to their photonic and excitonic components. At large times $t\to\infty$, $A_K(t)$ is only due to the contribution of the pole in the first sheet, cf. (37), because on one hand, the imaginary part of ξ^{II} is nonzero and negative and, on the other hand, $L_K(t)$ goes to zero as $1/t$, cf. (35). This result may be described in the following manner: Let $|\xi^I\rangle$, which is the pole of G_K located in the first Riemann sheet, be the discrete eigenstate of H (radiatively stable since $\mathrm{Im}\xi^I=0$). The projection of the initial state $|K\rangle$ on $|\xi^I\rangle$ increases suddenly when K crosses the intermediate region, cf. Figs. 12 and 13. If we write $|i(\omega)\rangle$

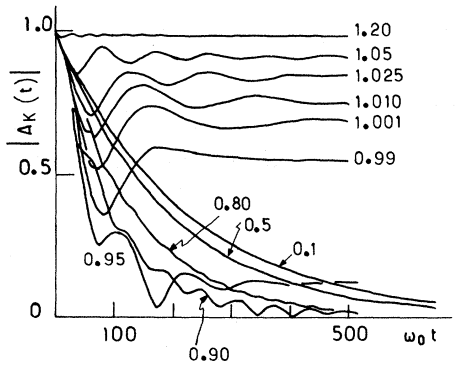

FIG. 11. Two-dimensional states: variation of the modulus of the probability amplitude $A_k(t)$ for different values of the ratio K/K_0 in the intermediate region. The time scale of the decay is of the order of 1 psec.

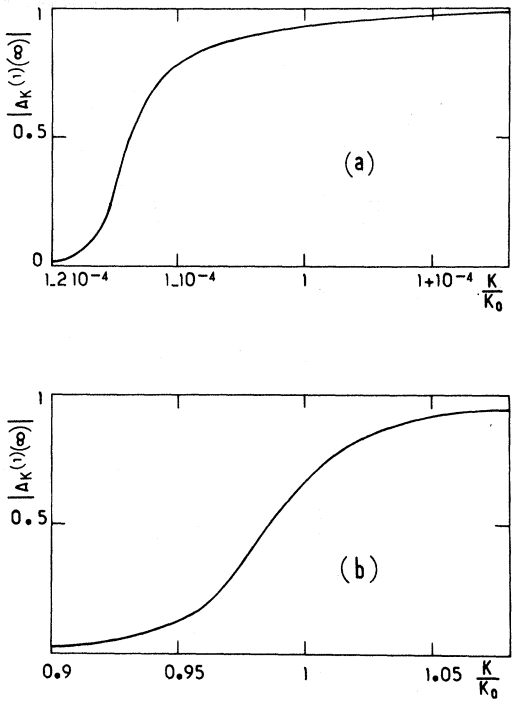

FIG. 12. Exciton character vs K of the polariton in one- and two-dimensional cases. We notice that the extension of the intermediate region is much larger for two-dimensional polaritons (b) than for one-dimensional polaritons (a).

for the continuum eigenstates of H, the general expression (17) may be written, separating the continuum and the discrete state contributions,

$$A_K^{(j)}(\omega)=|\langle K|i(\omega)\rangle|^2 g^{(j)}(\omega) + |\langle K|\xi_K^I\rangle|^2\delta(\omega-\omega_K^I)\,, \tag{38}$$

where $g^{(j)}(\omega)=0$ for $\omega<cK$. One may verify the completeness relation on the eigenstates of H.

$$A_K(t=0)=|\langle K|\xi^I\rangle|^2 + \int_{cK}^{\infty}|\langle K|i(\omega)\rangle|^2 g(\omega)\,d\omega=1\,.$$

As the first term in the right-hand side of (38) contains no δ peak, its contribution to $A_K(t)$ vanishes for $t\to\infty$. Then, using (36), we get

$$A_K(t\to\infty)=|\langle K|\xi^I\rangle|^2 = \left[1-\frac{1}{\hbar\omega_0}\frac{\delta R^I}{\delta\xi}\bigg|_{\xi^I}\right]^{-1}. \tag{39}$$

Using (22), one may check that $\delta R/\delta\xi\,|_{\xi^I}$ is necessarily negative. Furthermore, it is possible to re-

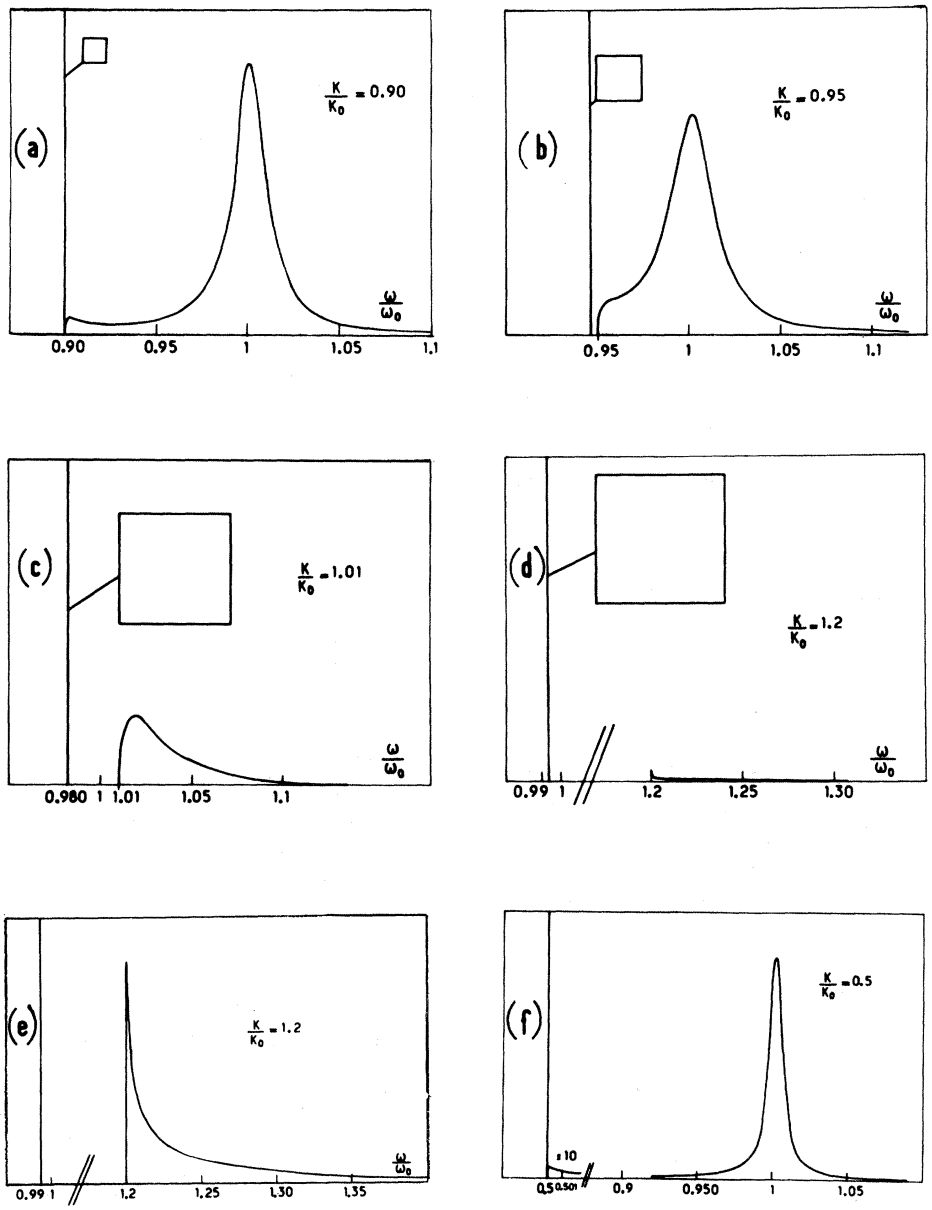

FIG. 13. Projection $A_K(\omega)$ of the matter state on the eigenstates of H in a two-dimensional system, for different values of $|K|$ and for $\theta=90°$. The vertical line stands for the stable polariton δ peak; the square indicates its area which may be compared to that of the excitonic resonance in the intermediate region [cf. (a)–(d)]. (e) indicates the shape of the resonance when the edge of the continuum is well above the exciton energy $\hbar\omega_0$, whereas (f) indicates the Lorentzian shape of the resonance where the edge is well below $\hbar\omega_0$.

late the excitonic character of the radiatively stable state to its dispersion curve, cf. Figs. 5 and 8. Indeed, in (22) $\ln(\mu-\xi)$ is the dominant term in the intermediate region $\mu\simeq 1$. Then one has the approximate relation:

$$\left.\frac{\delta R}{\delta\mu}\right|_{\mu} = -\left.\frac{\delta R}{\delta\mu}\right|_{\xi},$$

so that (39) becomes

$$|\langle K|\xi_K^I\rangle|^2 = 1-\frac{d\xi^{\mathrm{I}}}{d\mu} > 0\,. \tag{40}$$

Therefore, the variation of the matter character of the radiatively stable state, cf. Figs. 12(a) and 12(b), is directly related to its dispersion, cf. Figs. 5 and 8. In conclusion the state $|\xi_K^{\mathrm{I}}\rangle$ is practically

purely photonic for $K<K_0$ and purely excitonic for $K>K_0$. The change of the character occurs in the intermediate region whose extension $\Delta K^{(j)}$ strongly depends on the dimentionality ($\Delta K^{(j)} \simeq \Gamma^{(j)}_{K=0}/c$), where $\Gamma_{K=0}$ is the radiative width at $K=0$ of the radiatively unstable state, cf. Figs. 4 and 9. Again the index j indicates the dimension of the lattice. One may call the discrete state $|\xi^{\mathrm{I}}(K)\rangle$ a polariton of the molecular chain, or of the plane of molecules, by analogy with the three-dimensional case (its lower branch). For $K<K_0$, the polariton is a photonic mode trapped in the material system, and for $K>K_0$, the polariton is a downwards shifted exciton that is radiatively stable. With this polariton $|\xi^{\mathrm{I}}(K)\rangle$ dispersion (cf. Figs. 5 and 8, solid lines) is associated for $K<K_0$ a branch of radiatively unstable excitonic states $|\xi^{\mathrm{II}}(K)\rangle$, tentatively corresponding to the upper branch of the three-dimensional polariton, with the important difference that the energies $\xi^{\mathrm{II}}(K)$ are complex. The variations of $\hbar\omega_0 \mathrm{Re}\xi^{\mathrm{II}}(K)$ are plotted in Figs. 5 and 8 (broken lines) and the variations of $\hbar\omega_0 \mathrm{Im}\xi^{\mathrm{II}}(K)$ are plotted in Figs. 7 and 9. We indicate in dotted lines the variations when they have no physical meaning. In the intermediate region, where the excitonic unstable states lose their meaning, the description of the energy dynamics has to take into account the integral $L_K(t)$. We notice, however, that the derivation of the polariton states is not affected by $L_K(t)$ since this quantity may be neglected for $t\to\infty$. The spectral broadening of a two-dimensional excitation is illustrated in Fig. 13. Anomalous with respect to a resonance Lorentzian line shape, the spectral line shapes in Fig. 13 are counterparts of nonexponential, noncomplete radiative decays illustrated in Fig. 11.

D. Discussion

In this subsection, we review briefly features which are proper to a collective excitation-radiation interaction, to its successive approximations, and also features which are specific to the dimensionality.

The results obtained by the pole approximation for the two dimensions of the lattices account correctly for the essence of the phenomenon outside of the intermediate region, shift of a purely real energy level for $K>K_0$, shift and radiative width for $K<K_0$, cf. Figs. 3, 4, 6, and 7. This behavior is easily understood in terms of a discrete state $|\hbar\omega_0\rangle$ coupled to a continuum. When the lowest state of the continuum is above $\hbar\omega_0$, i.e.,

$$[\hbar(K^2+q^2)^{1/2}]_{q=0}>\hbar\omega_0$$

the continuum repels downwards the discrete state with a negative shift. On the contrary when $\hbar cK<\hbar\omega_0$, the discrete state overlaps the continuum and is mixed with it, cf. also Fig. 2. In the intermediate region Δ and Γ vary very rapidly and this excludes the validity of the pole approximation [Δ shows logarithmic divergence for one-dimensional systems, Δ and Γ show more severe divergence, as $(K^2-K_0^2)^{-1/2}$, for two-dimensional systems].

In the region $K<K_0$, $\Delta_K^{(j)}$ and $\Gamma_K^{(j)}$ take values which are $(\lambda/a)^{(j)}$ times larger than the corresponding quantities for a single site; this amplification of the interaction shows the trend of a collective excitation to exhibit constructive (short radiative processes) and destructive (long radiative processes) effects in the interactions between sites. The decay probability of the collective excitations of the N molecules in the molecular chain or in the plane of molecules is redistributed over the exciton states $0\le K\le(\omega_0/c)$. Thus we have superradiant-like states for $K\le\omega_0/c$, accompanied by subradiant states for $K>\omega_0/c$, with $\Gamma=0$. With respect to the redistribution of the radiative decay probability on the exciton states, it is interesting to notice that analysis of the trace of the self-energies, cf. (19) and (30), shows that for a system of $N^{(j)}$ molecules, in the pole approximation, one has the relation

$$\sum_K \Gamma_K^{(j)}=N^{(j)}\Gamma^{(0)} . \tag{41}$$

The introduction of the exact poles in the resolvent, cf. Figs 5, 8, and 9, shows that there are no significant changes outside the intermediate region. On the contrary, the abnormal behavior of the radiative interactions disappears in that region. The sudden changes that Γ and Δ show for $cK>\omega_0+\Delta(K_{\mathrm{cr}})$ are contributions from $\xi^{\mathrm{II}}(K)$; they have no physical meaning, cf. dotted lines in Figs. 8 and 9.

In conclusion, the main reason of the failure of the pole approximation to describe the interaction in the intermediate region, is that by putting in the zeroth order $z=(\hbar\omega_0+i\epsilon)_{\epsilon\to 0}$, one makes a perturbation treatment and assumes that the excitonic and photonic components may be distinguished

separately. In the intermediate region these components are comparable and the perturbation treatment fails. As for the stability of the initial state $|\vec{K};0\rangle$ coupled to a continuum of photons of arbitrary extension, cf. Figs. 11 and 13, we find the two-limit behavior for which the pole approximation is valid. (i) For $0 \leq K \ll K_0$, the discrete state faces a continuum without singularities and is mixed into it, so that $A_K(t)$ decays exponentially. (ii) For $K \gg K_0$, the discrete state is repelled downwards without mixing $|A_K(t)|$ remains constant. In the intermediate region where the discrete state faces a continuum near a singularity, the decay is neither forbidden, as it is for $K \gg K$, nor total as for the case $K \ll K_0$. In this region, the two poles contribute and interfere; this explains the oscillating behavior of the excitonic component with beats of frequency $|\Delta_K^{\mathrm{I}} - \Delta_K^{\mathrm{II}}|$. However, unlike the three-dimensional case where each exciton $\vec{K}$ "faces" a single photon $\vec{k}$ with $\vec{k} = \vec{K}$ and where these oscillations are not damped, in one- and two-dimensional cases the effective continua $g^{(1)}(\omega)$ and $g^{(2)}(\omega)$ introduce a radiative damping mechanism for the excitonic component, this damping being stronger for a two-dimensional excitation. The behavior of the excitonic component is better understood when we consider its smearing out into the spectrum of the total Hamiltonian. In Fig. 13, the square on the discrete polariton state indicates the excitonic component, i.e., $|\langle \vec{K} | \xi_K^{\mathrm{I}} \rangle|^2$, which survives in the polariton state after complete decay. The line shape of the continuum measures the spectral density of the state $|\vec{K},\hbar\omega_0;0\rangle$ at the energy $\hbar\omega$, i.e.,

$$A_K(\omega) = |\langle \vec{K} | i(\omega) \rangle|^2 g(\omega) .$$

When one may neglect the variation of $g(\omega)$ over the width of the peak of $A_K(\omega)$, then the spectral line is a Lorentzian and the decay $A_K(t)$ is exponential. On the contrary, when the unperturbed state $|\vec{K},\hbar\omega_0;0\rangle$ approaches the singularity of the continuum, the spectral line around the maximum becomes non-Lorentzian and asymmetric. Such a spectral shape corresponds to a nonexponential decay of $A_K(t)$, complicated by the beats of the resonance with a polariton state which exhibits, in this region, an excitonic amplitude comparable to that of the continuum, cf. Figs. 13(b) and 13(c).

1. *Dimensionality effects*

The dimensionality shows up strongly in two quantities, the radiative shift and the extension of the intermediate region where the states are superpositions of photons and excitons. For instance, when we compare the self-energies $R^{(1)}$ and $R^{(2)}$, cf. (19) and (30), respectively, we find that the radiative widths in systems of dimension 2, 1, and 0 are simply related.

$$\Gamma^{(2)} \simeq \left[\frac{\lambda}{a}\right] \Gamma^{(1)} \simeq \left[\frac{\lambda}{a}\right]^2 \Gamma^{(0)} . \tag{42}$$

Although the mathematics of this relation are clear, one may interpret this relation by saying that although the two-dimensional excitation faces a less dense effective continuum $g^{(2)}(\omega)$ than the one-dimensional excitation, it exhibits a much stronger transition dipole, so that the final coupling is stronger than that of the one-dimensional excitation. Also, analyzing expression (40) one finds that the extension of the intermediate region $\Delta K^{(j)}$ is larger for the two-dimensional excitation than for the one-dimensional excitation. One obtains

$$\Delta K^{(2)} \simeq \left[\frac{\lambda}{a}\right] \Delta K^{(1)} . \tag{43}$$

This relation shows once again the role of the dimensionality in the interaction of excitations with radiation, cf. Figs. 12(a) and 12(b).

V. THE THREE-DIMENSIONAL CASE

The three-dimensional lattice is assumed infinite in all three directions. Thus photons and excitons are quantized in the same box of L^3 where L goes to ∞. In this case, there is no exciton state facing a continuum of photons but in each subspace K there are two excitons with momenta $\vec{K}$ and $-\vec{K}$, and photons with moment $\vec{K}$ and $-\vec{K}$, and the effective continuum is of dimension zero.

A. The quasiboson approximation

The three-dimensional case has been treated in a straightforward manner by adopting boson statistics for excitons as well as for photons.[15–17] This is a harmonic oscillator approximation in the limit of weak excitation, i.e., valid for low density of excitons. The following equation has been derived[1,16] for real eigenenergies $\hbar\omega(K)$ in the subspace K.

$$[z^2 - (\hbar\omega_0)^2][z^2 - (\hbar\omega_K)^2] = 4\omega_0\omega_K\hbar^2 |\langle \vec{K};0 | H_I | 0;\vec{K},\vec{\epsilon} \rangle|^2 , \tag{44}$$

with

$$|\langle K;0|H_I|0;\vec{K},\vec{\epsilon}\rangle|^2=\frac{2\pi N\hbar}{L^3}\frac{\omega_0^2}{\omega_K}|\vec{\epsilon}\cdot\vec{D}|^2,$$

$$\omega_K=cK .$$

These eigenstates correspond to new quasiparticles, the polaritons, which are combination of photons and excitons and diagonalize the total Hamiltonian (1) written in the quasiboson approximation,

$$H=\sum_{K,\nu}z_{K\nu}C_{K\nu}^{\dagger}C_{K\nu}+\Delta\epsilon ,$$

with

$$C_{K\nu}=U_K^{\nu}B_K+V_K^{\nu}B_K^{\dagger}+\sum_{\epsilon}(U_{K\epsilon}^{\nu}a_{K\epsilon}+V_{K\epsilon}^{\nu}a_{K\epsilon}^{\dagger}),$$

where $B_K,B_K^{\dagger}$ and $a_{K\epsilon},a_{K\epsilon}^{\dagger}$ are Bose operators for excitons and photons, respectively. The coefficients U_K and V_K represent the weight of the excitonic state in the eigenstate of H and show the change of the character of the eigenstate when the momentum passes through the intermediate region.[1] Such changes have been discussed for one- and two-dimensional polaritons, cf. Figs. 12(a) and 12(b). The results (44) are exact in the quasiboson approximation in the sense that they sum up all orders of the perturbation H_I. On the other hand, it is obvious that the assumption of bosons is not equivalent to the method we used in Sec. III, for one- and two-dimensional lattices, using a Feynman propagator for photons and a two-level approximation for the excitonic state.

B. Calculation of three-dimensional polaritons with Feynman propagators

We wish to show that it is possible to arrive at the exact results (44) by extending to the three-dimensional case the technique of Feynman propagators we used for systems of lower dimension. Let us first notice that using Feynman propagators for photons only, one arrives at the result,

$$z=\hbar\omega_0+R_F^{(3)}(z)=\hbar\omega_0+2\hbar\omega_K\frac{|\langle\vec{K};0|H_I|0;\vec{K},\vec{\epsilon}\rangle|^2}{z^2-(\hbar\omega_K)^2}, \quad (45)$$

which approaches that of (44). Now since in the boson approximation excitons and photons obey Bose statistics, we associate in our technique the same type of Feynman propagators to photons and to excitons, $2\hbar\omega_K/(z^2-\hbar^2\omega_K^2)$ and $2\hbar\omega_0/(z^2-\hbar^2\omega_0^2)$, respectively. Thus in our calculation of the restricted resolvent PGP, we replace in (10a),

$$PG_0P=\frac{P}{z-H_m}=\frac{P}{z-\hbar\omega_0} \text{ by } P\frac{2\hbar\omega_0}{z^2-\hbar^2\omega_0^2}, \quad (46)$$

and we arrive at the implicit equation (44) by seeking the poles of PGP in (10a). The fact that we obtain the same result with the method of Feynmann propagators suggests the following equivalence of the mathematical techniques: (i) The quasiboson approximation is equivalent to the approach of associating Feynman propagators to photons and to excitons in a two-level approximation. (ii) Correlatively, in systems of two particles, Feynman propragators sum up all orders of the perturbation H_I. Such an equivalence is implicit in works of many authors investigating the interaction of electrons with bosons (photons or phonons); see, for instance, Ref. 8.

VI. CONCLUSION

By using translational symmetry and neglecting the atomic structure of matter, we showed that the study of the coupling to radiation of a one- or two-dimensional exciton reduces to that of a discrete matter excitation, of wave vector K and energy $\hbar\omega_0$, coupled to an effective photon continuum which has a low-energy edge $\hbar c|K|$. The coupled system essentially presents two kinds of limiting behavior according to the position of the excitonic energy $\hbar\omega_0$ relative to the low-energy edge of the effective continuum.

(i) When $K>\omega_0/c$, the matter excitation is simply repelled downwards. Thus it is radiatively stable (the polariton).

(ii) When $K<\omega_0/c$, the matter excitation is radiatively unstable (the radiatively unstable exciton).

These two behaviors reflect the cooperative trend in the coupling to the photon of the site dipoles of the exciton. These cooperative effects lead to subradiant[18] states for $K>\omega_0/c$ and to superradiant states for $K<\omega_0/c$, with an amplifying factor $(c/\omega_0 a)^d$ for the d-dimensional exciton radiative decay.

The transition between these two responses to the coupling to the radiation, which occurs around $K\simeq\omega_0/c$, has been thoroughly investigated. The behavior in the transition region is well known for

three-dimensional lattices, where, for each wave vector K, two discrete eigenstates are formed (real eigenenergies) as superpositions of exciton and photon. In one- and two-dimensional coupled systems, the eigenstates are, on the one hand, a discrete state of mixed character (the so-called d-dimensional polariton) and, on the other hand, the photon continuum mixed with matter character showing non-Lorentzian shape in the transition range of wave vectors K. Correlatively, the time evolution of the matter excitations shows an incomplete decay into the photon continuum, with oscillations between the polariton and the excitonic resonance.

The systems we investigated have allowed us to present, from the theoretical point of view, an example of discrete state coupled to a continuum of photons near an edge. In addition, the quantum-mechanical model we developed to investigate the cooperative emission in two-dimensional exciton states is a prerequisite for an investigation of surface or bulk radiative dynamics in crystals of layered structure, such as anthracene, which we will present in part II of this series.

---

*Present address: Groupe de Physique Solides des l'Ecole Normal Superieure, Universite de Paris VII, 75221 Paris, France.

†Laboratory associated with CNRS (LA 283).

[1]J. J. Hopfield, Phys. Rev. 112, 1555 (1958).

[2]U. Fano, Phys. Rev. 103, 1202 (1956); S. I. Pekar, Zh. Eksp. Teor. Fiz. 33, 1022, (1975) [Sov. Phys.—JETP 6, 785 (1958)]; V. M. Agranovitch, Zh. Eksp. Teor. Fiz. 37, 340 (1959) [Sov. Phys.—JETP 10, 307 (1960)].

[3]V. M. Agranovitch and O. A. Dubovskii, Zh. Eksp. Teor. Fiz. Pis'ma Red 3, 345 (1966) [JETP Lett. 3, 223 (1966)].

[4]M. R. Philpott and P. G. Sherman, Phys. Rev. B 12, 5381 (1975).

[5]M. R. Philpott, J. Chem. Phys. 63, 485 (1975).

[6]J. M. Turlet and M. R. Philpott, J. Chem. Phys. 64, 3852 (1976).

[7]J. M. Turlet, J. Bernard, and P. Kottis, Chem. Phys. Lett. 59, 506 (1978), and references therein.

[8]J. M. Ziman, *Elements of Advanced Quantum Theory* (Cambridge University Press, London, 1969).

[9]K. E. Jones and A. H. Zewail, in *Advances in Laser Chemistry,* Vol. 3 of *Springer Series in Chemical Physics,* edited by V. I. Goldanskii, R. Gomer, F. P. Schäfer, and J. P. Toennies (Springer, Berlin, 1978), p. 196.

[10]M. K. Grover and R. Silbey, J. Chem. Phys. 52, 2099 (1970); 54, 4843 (1971).

[11]U. Fano, Phys. Rev. 124, 1866 (1961).

[12]The problems of particle statistics originating from the existence of two excitons with the same wave vector $\vec{K}$ are disregarded here. They can be solved by a quasiboson approximation for excitons (see Sec. V, and Refs. 16–18 here below).

[13]C. Cohen-Tannoudji (unpublished).

[14]B. S. Sommer and J. Jortner, J. Chem. Phys. 50, 187 (1969); 50, 839 (1969).

[15]S. V. Tyablikov, *Methods in the Quantum Theory of Magnetism* (Plenum, New York, 1967).

[16]A. S. Davydov, *Theory of Molecular Excitons* (Plenum, New York, 1971).

[17]H. Freedhof and J. Van Kranendonk, Can. J. Phys. 45, 1833 (1967).

[18]The terms subradiant and superradiant are not to be taken here in the exact sense of Dicke [R. J. Dicke, Phys. Rev. 93, 99 (1954)] since only one excitation is involved in the system of dipoles. Rather, they refer to the absence or to the rapidity of the decay compared to that of a single dipole.